

# PAW: a Hybrid Wheeled-Leg Robot

James Andrew Smith  
Centre for Intelligent Machines  
McGill University  
Montréal, Québec, Canada  
Email: jasmith@cim.mcgill.ca

Inna Sharf  
Centre for Intelligent Machines  
McGill University  
Montréal, Québec, Canada  
Email: inna.sharf@mcgill.ca

Michael Trentini  
Autonomous Intelligent Systems Section  
Defence R&D Canada – Suffield  
Medicine Hat, Alberta, Canada  
Email: Mike.Trentini@drdc-rddc.gc.ca

**Abstract**— This paper discusses current wheeled mobility work on a hybrid wheeled-leg robot called PAW. In addition to providing design details, controllers are proposed for inclined turning and sprawled braking which take advantage of the hybrid nature of the platform and improve stability. Power consumption values for a number of its basic behaviours are given, as is the range of the robot.

## I. INTRODUCTION

### A. Small/Medium Wheeled and Tracked Mobile Robots

Designers of ground-based mobile systems tend to create vehicles which use wheels or tracks for locomotion for a number of reasons. These vehicle designs can take advantage of a large accumulated knowledge base, very good performance characteristics, and established methods for maintenance, construction and manufacturing, [1] - [3]. These vehicles offer an efficient and often rapid method of ground traversal, especially in conditions where the terrain is flat. Of particular relevance to the mobile robotics community, a number of studies have been performed on relatively small tracked or wheeled platforms (e.g. [4] and [5]), of which iRobot's Packbot [6] is one of the more successful and widely deployed examples.

### B. Legged Robots

As mobile robots are required to operate in more challenging environments, the limitations of traditional wheeled and tracked vehicle designs become increasingly apparent: their simple and robust design does not provide sufficient versatility and adaptability for many real-world terrain conditions. Design modifications, which add passive or active degrees of freedom with or without compliance, can be made to make these vehicles better suited to rough terrain. Packbot's foot-like tracked paddles and NASA's Sojourner rover's bogies [7] are examples of modifications made to traditional tracked and wheeled vehicles that have enabled greater mobility.

An alternative to traditional wheeled and track designs is the leg. The biological world is filled with a multitude of inspirational yet *complex* examples of legged locomotion. Although not as broad as the literature available for wheeled or tracked vehicles, knowledge about the analysis and synthesis of legged systems is available, [8] - [10]. In general, legged systems are more complex, less efficient, have smaller operational ranges, and have higher peak power and torque requirements than wheeled and tracked systems. In addition, their payloads and sensors must withstand or compensate for oscillatory motion.

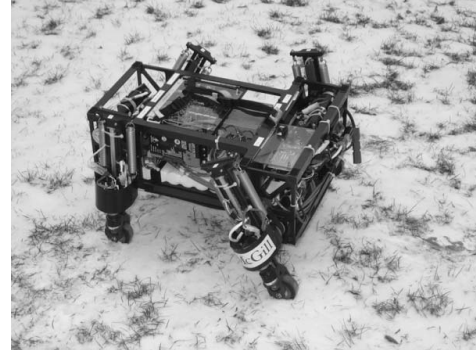


Fig. 1. The PAW Robot

For all of these disadvantages legs still have potential advantages. Biological examples of legged systems that readers are familiar with reinforce the notion that legs provide versatility, redundancy and potential adaptability that simple wheeled and tracked systems cannot. Wheeled and tracked vehicles require, for the most part, continuous contact surfaces whereas legged systems can locomote on terrain with isolated footholds. Legged robots, such as those in the RiSE project, can be designed specifically for environments where foothold selection is critical, such as vertical surfaces, [11]. In addition, artificial legged systems are no longer limited to quasi-static motion, as was demonstrated in the 1980s at the CMU and MIT Leg Labs where simple controllers were made to stabilize high speed motion of monopedal, bipedal and quadrupedal robots, [10]. Even simpler controllers for high speed quadrupedal locomotion have recently been implemented on the Scout II robot, [12]. The six-legged RHex platform, [13], was shown to be nearly as capable as the commercially developed PackBot platform under difficult outdoor conditions, [5].

### C. Articulated Suspension Systems

It is possible to obtain many of the advantages of both traditional wheeled and legged systems by combining aspects of these into a single articulated suspension platform. The Roller-Walker robot, [16], has demonstrated that passive wheels attached to the distal ends of actively-controlled legs can allow a vehicle to roll along a surface. The Shrimp system negotiates terrain with actuated wheels and a passive adaptation mechanism, [14]. In contrast, the Hylos system uses active posture control to adapt to irregular terrain in order to maintain stability and traction, [15].

#### D. The PAW Robot: a Hybrid Wheeled-Leg System

The PAW (Platform for Ambulating Wheels) robot, as pictured in Fig. 1, like other articulated suspension systems, combines aspects of legged and wheeled locomotion in order to achieve greater mobility. This paper describes primarily kinematic wheeled aspects of PAW's locomotion behaviours, but the results have implications for high speed locomotion in which vehicle dynamics play a role, such as in braking and high speed turning. PAW uses a lighter and more compact version of Scout II's T-shaped body. Unlike Scout II, the legs are capable of limited recirculation and are equipped with actuated hard rubber wheels instead of fixed toes. In wheeled modes of operation the four hip motors can reposition the wheels with respect to the body of the robot. In legged modes the wheels are actively locked, allowing dynamic behaviours such as jumping and bounding, as suggested in the simulations presented in [17].

The Autonomous Intelligent Systems Section at Defence R&D Canada – Suffield (DRDC Suffield) envisions autonomous systems contributing to homeland security, search and rescue, and peacekeeping roles abroad. On the ground, Uncrewed Ground Vehicles (UGVs) will be called upon to enter unknown city blocks to keep soldiers out of harm's way. They will need to navigate unknown complex environments, providing information with sufficient detail for tactical operations and contribution to real-time situational awareness. However, the mobility of ground-based mobile systems operating in urban settings must increase significantly if robotic technology is to augment human efforts in these roles and environments.

DRDC Suffield is exploring novel mobile platforms that use intelligent mobility algorithms to improve robot mobility in unknown highly complex terrain. These algorithms seek to exploit available world representations of the environment and the inherent capabilities of the platform to allow the robot to interact with its surroundings and to locomote. This research addresses the utility of UGVs if they are to be used in military relevant roles and environments. To be effective, the UGV must provide situational awareness and carry equipment

TABLE I  
PAW BODY PARAMETERS

Parameter	Value
front body width	0.366 m
rear body width	0.240 m
front wheel-to-wheel width	0.478 m
rear wheel-to-wheel width	0.352 m
body length	0.494 m
hip separation	0.322 m
wheel diameter	0.066 m
leg length	0.212 m
body height	0.170 m
max body clearance	0.124 m
leg mass (each)	1.2 kg
body mass	15.7 kg
m. of inertia ( $I_{xx}, I_{yy}, I_{zz}$ )	(0.16977, 0.46939, 0.37171) kg m <sup>2</sup>
pr. of inertia ( $I_{xy}, I_{xz}, I_{yz}$ )	(0.00061, -0.00064, 0.00665) kg m <sup>2</sup>
leg spring constant	2000 - 3200 N/m

at a tempo that enhances the performance of the Canadian Forces. While the wheeled mechanism addresses this necessity, the compliant leg aspect yields obstacle-overcoming dynamic behaviours. The mobility characteristics of robots designed in this manner, combined with intelligent mobility algorithms, will outperform larger systems without these capabilities.

The PAW robot addresses the need for a UGV to transition from operation in relatively simple environments (composed of streets, sidewalks, trees, bushes) into more complex environments (that include trenches, berms, abandoned vehicles, rubble, wire barricades) and finally into highly complex environments (with sewers, tunnels and buildings with tight confines and obstacles designed on a human scale).

## II. DESIGN OF PAW, A HYBRID WHEELED-LEG SYSTEM

### A. Mechanical and Electrical Design

PAW has been designed as a platform for the study of both wheeled and dynamically stable legged modes of locomotion and to be power and computationally autonomous.

1) *Mechanical Components*: The body of the robot consists of a T-shaped aluminum frame for which the basic parameters are listed in Table I. The hip joints of the four legs are each driven by a 90 Watt Maxon 118777 brushed DC motor. The motors contain 73.5:1 gearheads and quadrature encoders with 2000 counts-per-revolution effective resolution. A toothed belt and pair of sprockets provide a further 32:24 reduction ratio. Each leg is equipped with a pair of extension springs rated of up to 3200 N/m. At the end of each leg is a 20 Watt Maxon 118751 brushed DC motor with a 4.8:1 Maxon 233147 planetary gearbox and a custom 3:1 ratio bevel gear pair connected to a 0.066 m diameter wheel. The wheel motors' quadrature encoders are identical to those of the hip motors.

In contrast to the original design, [17], which emphasized hip speed, selection of the current planetary gearbox and pulley combination was made to maximize available hip torque. The availability of high hip torque is especially important when the robot stands up or carries a payload.

Power and signal wires to the motors and sensors on each leg are passed through a hollow hip axle. This prevents the cables from becoming entangled in the legs and results in a simpler and more compact solution than that which can be provided with conventional commercial slip rings. Unfortunately, this prevents the legs from continuously recirculating, as is the case in robots such as RHex.

2) *Electrical Components*: Apart from the motors described earlier, other relevant electrical components on the robot include a PC/104 computer stack, four AMC 25A8 brushed DC motor amplifiers for driving the hip motors, a custom amplifier board containing Apex SA60 motor amplifiers and three NiMH battery packs.

The PC/104 computer stack contains a Pentium-compatible processor board running the QNX 6.1 real-time operating system and control code, a PCMCIA board with wireless Ethernet card for teleoperation, a power supply board, a quadrature decoder board for obtaining motor angles and two I/O boards, one custom and the other off-the-shelf.

The AMC amplifiers are set to deliver 10 A of continuous, 20 A peak, current to each hip motor, while the Apex amplifiers can deliver 10 A continuous, 15 A peak to each wheel motor.

Two different sets of NiMH battery packs, made up of industry standard D-cells, are used. The Twicell HR-D packs are manufactured by Sanyo, while the VH D cells are manufactured by Saft. The Sanyo Twicells have a charge capacity of up to 7.5 Ah, while the Saft VH D cells have a charge capacity of up to 9.5 Ah.

3) *Proprioceptive Sensors*: The PAW robot houses very few sensors. In addition to battery voltage and current sensors, the robot uses one quadrature encoder with 2000 counts per revolution effective resolution in each of its eight motors, one linear potentiometer with up to 0.10 m range in each of its four legs and a current sensor on each hip motor amplifier.

The motor encoders are used to determine the angle of the eight motor shafts, while the linear potentiometers are used to measure leg compression. By measuring current consumption and battery voltage it is possible to determine power usage in various subsystems of the robot. In the case of the hip motor amplifiers current measurement provides a proportional estimate of motor torque applied to the hip.

### B. Motor Control Design

Control of the wheeled behaviours presented in this paper is achieved through the use of proprioceptive encoder sensors on each motor and voltage and current sensing only.

At the heart of the control for each joint of the robot is a proportional-integral-derivative (PID) controller which is responsible for either maintaining a desired position or a desired velocity at that joint. The equation for position control of a particular joint is described as:

$$\tau_{desired} = k_p \Delta_{position} + k_i \Sigma \Delta_{position} + k_d \Delta_{velocity} \quad (1)$$

where  $\tau_{desired}$  is the desired motor torque,  $\Delta_{position}$  is the error between actual and desired motor position/angle,  $\Delta_{velocity}$  is the error between actual and desired motor angular velocities,  $\Sigma \Delta_{position}$  is the accumulated error in motor position/angle, and  $k_p$ ,  $k_i$  and  $k_d$  are the proportional, integral and derivative gains, respectively.

The desired motor torques are converted into control signal voltages which are then fed into one of two types of amplifiers. AMC 25A8 amplifiers are used in closed-loop current/torque control mode for the hips, while an amplifier board housing Apex Microtechnology SA60 amplifiers is used to drive the wheel motors. The control signal voltage for the hip amplifiers is set to be proportional to the desired amplifier current using the manufacturer-specified conversion factor, while the resulting amplifier current is directly related to the motor shaft torque using conversion factors and efficiency values provided by Maxon Motors. The SA60 amplifiers are essentially open-loop PWM amplifiers, unlike the AMC 25A8s. By estimating current draw by the wheel motors it is possible to obtain a

reasonable estimate of the applied torque at each wheel. Details on motor current estimation without direct measurement, using a motor model, battery voltage measurements and motor speed measurements, are explained in [18].

In the case of controlling a desired position, such as during braking, a desired position value is given and the desired velocity is set to zero. In the case where the controller is required to maintain a particular velocity, a constant desired velocity is set and a matching desired position trajectory is computed. Alternatively, a PID velocity controller can be set up using wheel velocity error,  $\Delta_{velocity}$ , and accelerations,  $\Delta_{acceleration}$ , (desired acceleration is 0) to command an amplifier control voltage,  $V_{DAC}$  proportional to the battery voltage but without the use of a motor model, as follows:

$$V_{DAC} = k_p \Delta_{velocity} + k_i \Sigma \Delta_{velocity} + k_d \Delta_{acceleration}. \quad (2)$$

Transitions between one set of desired velocities and/or positions and another is resolved using cycloidal functions, [19], which provide smooth motion and are relatively computationally efficient.

Because the robot is redundantly actuated and there is no coordination between individual motor controllers during wheeled locomotion it is not possible to have overly high gains on all joints. High gains are set on the hip actuators to ensure that the wheels are properly positioned with respect to the body and lower gains are used at the wheels, resulting in relatively compliant wheel motion. This active compliance tends to smoothen wheel velocity transitions.

### III. TURNING AND BRAKING CONTROLLER DESIGN

Two types of controllers are introduced in this section. The first describes a method for turning, while the second describes a method for braking. Both controllers take advantage of the ability to reposition the wheels with respect to the body of the robot.

1) *Inclined Turning Controller*: Turning of the robot is achieved through a modified version of the standard differential/skid steering approach. Rather than applying differential wheel speeds on either side of the robot with the legs fixed, the legs are used to reposition the wheels to reduce shear forces on them. Effectively, this means that while the legs on the outside of the turn are kept vertical with respect to the body, the legs on the inside of the turn are brought together, lowering the centre of mass (COM) and leaning the robot *into* the turn.

The following calculations approximate the robot body as a rectangular box. The wheels are assumed to move in a plane flush with the edge of this box. These two planes are located on each side of the the real robot's T-shaped body, halfway between the wheels. For this model, the body width,  $W$ , is taken to be 0.415 m, midway between the two wheel-to-wheel widths mentioned in Table I.

Given a desired turning radius for the ground-projected centre of mass, two concentric circles are determined which share the same centre as the turning radius of the COM but which intersect either the inner or outer wheel pairs. Wheel

speed is then set in a proportional fashion to the desired ground-project centre-of-mass speed.

Given a desired COM height,  $H$ , a known maximum leg length,  $l$ , a known body width,  $W$ , and a requirement that one pair of legs must remain vertical with respect to the body's local coordinate frame, a roll angle,  $\varphi$ , can be determined:

$$\varphi = \text{acos}\left(\frac{H}{\sqrt{l^2 + \frac{W^2}{4}}}\right) + \text{atan}\left(\frac{2l}{W}\right) - \frac{\pi}{2}. \quad (3)$$

Next, the height of the hips of the inner legs,  $h$  can be determined:

$$h = l \cos(\varphi) - W \sin(\varphi). \quad (4)$$

The angle,  $\phi$ , at which the hip angle is set with respect to the body can now be calculated:

$$\phi = \text{acos}\left(\frac{\frac{h}{\cos\varphi} - w_r}{l'}\right) \quad (5)$$

where  $w_r$  is the radius of the wheel and  $l'$  is the length of the leg from the hip to the wheel axle,  $l - w_r$ . The second hip's angle is simply set to  $-\phi$ , resulting in the inner hips being in a tucked configuration, as seen in Fig. 2a.

In order to determine the inner and outer turning radii, one must determine the location of one of the wheels in the inner pair and one in the outer pair with respect to the COM of the robot, where the  $x$  and  $y$  axes form a plane parallel to the ground, whose origin is located directly below the COM:

$$x_{inner} = -l' \sin(\phi) + k \quad (6)$$

$$y_{inner} = -\frac{W}{2} \cos(\varphi) + h \tan(\varphi) \quad (7)$$

$$x_{outer} = k \quad (8)$$

$$y_{outer} = \frac{W}{2} \cos(\varphi) + l \sin(\varphi) \quad (9)$$

where  $k$  is half the hip spacing. Given a desired turn radius for the COM,  $r_{COM}$ , the turn radius for the inner legs can be found as follows:

$$r_{inner} = \sqrt{(x_{inner})^2 + (-y_{inner} + r_{COM})^2} \quad (10)$$

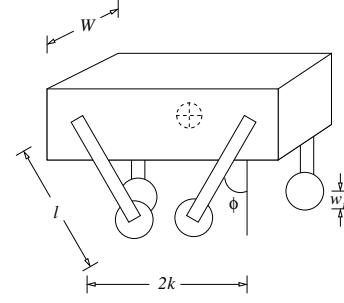
while the turn radius for the outer legs is

$$r_{outer} = \sqrt{(x_{outer})^2 + (y_{outer} + r_{COM})^2}. \quad (11)$$

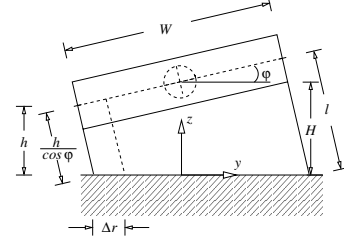
To set the speed of the wheels on the T-shaped layout of the real robot, the inner and outer radii are corrected by  $\pm\Delta r$  to account for the offsets between front and rear wheels with

$$\Delta r = \frac{1}{4} \frac{\Delta W}{\cos\varphi} \quad (12)$$

where  $\Delta W$  is the the difference in front and rear "wheel to wheel" widths on the robot, as listed in Table I. The wheel speeds are set proportionally to the corresponding radii to give the desired COM speed.



(a) Three-Quarter View



(b) Frontal View

Fig. 2. Simplified views (rectangular vs. T-shaped) of PAW illustrating some important variables used in calculating hip angles for the turning algorithm.

2) *Sprawled Braking Controller*: Another important aspect of PAW's locomotion that must be considered is stopping. While driving forwards or backwards it is important to apply braking action in such a way as to prevent the robot from pitching over. Pitching motion can result from braking too suddenly or by angling the legs either vertically or in a tucked configuration. During forward and reverse driving the robot places its legs in a sprawled posture, at about  $\pm 11.5$  degrees with respect to the body's vertical reference. When a brake command is issued the motors are used to dissipate the kinetic energy of the robot through the use of low gain PID controllers, as described in Section II-B, which also prevent wheel slip.

#### IV. EXPERIMENTAL RESULTS

In this section experimental results will be presented and discussed. Four basic results have been obtained, including a maximum cruising speed of 2.0 m/s, an operational range of over 2500 m achieved in approximately one hour, turning tests with radii from 0.5 to 1 m, and a demonstration of a sprawled rolling and braking posture which aids stability.

##### A. Cruising Speed Experiments

The highest straight-line speed attempted on the robot to date is 2.0 m/s, matching the predicted maximum rolling velocity discussed in [17].

For mobile robots to be of practical utility, they need to be energy efficient and be able to operate in a power autonomous fashion for extended periods of time. One measure of energy efficiency, as described in [20], is the specific resistance,

$$\epsilon(v) = \frac{P(v)}{mgv}$$

where  $P$  is the power expenditure,  $m$  is the mass of the vehicle,  $g$  is the gravitational acceleration constant, and  $v$  is the vehicle speed. Power consumption can be determined using onboard voltage and current sensors. While sitting with its body against the ground the robot has an average quiescent power consumption of 25 W. Comparatively, when placed on a 16 degree slope, with its legs locked perpendicular to its body and its wheels in active brake mode the robot consumes approximately 58 W.

Power consumption has also been measured for the robot rolling in a straight line at constant speed. At a speed of 1.4 m/s its average power consumption has been found to be 51 W, while at 2.0 m/s it is 56 W. This corresponds to a specific resistance of 0.18 at 1.4 m/s and 0.14 at its current maximum speed, indicating that the robot runs more efficiently at the higher speed. In comparison, legged robots such as Scout II have an unsurprisingly higher specific resistance: 1.4 while bounding at 1.3 m/s, [12], and 1.47 while galloping at 1.4 m/s, [22].

### B. Operational Range

The robot uses three battery packs composed of a total of 30 NiMH D-Cells, as discussed earlier. At its current maximum speed of 1.4 m/s the robot draws approximately 1.36 A, yielding a peak theoretical run-time of over five hours using the HR-D and nearly seven hours with the VH D battery packs. On flat ground this translates to a maximum theoretical distance of 28 to 35 kilometres, respectively. To test the maximum range of the robot under somewhat more realistic conditions than non-stop straight line motion, the robot was made to move back and forth on a three metre track with a maximum desired speed of 1.4 m/s until a critical (below 32 VDC) battery voltage was detected. Using a set of the VH D battery packs the robot travelled a total of 2562 m in 59 minutes, with four brief interruptions to check motor temperature. The test was terminated when the battery voltage dropped suddenly from above 32 VDC to 21 VDC during a deceleration. In order to increase operational range the frequency of direction-of-travel changes could be lowered, deceleration and acceleration phases could be increased in length to decrease maximum current draw in the wheels, and the legs could be positioned more vertically to reduce current draw to the hip motors.

### C. Turning

A series of tests were conducted on the turning behaviour, as described in Section III. Wheel control is based on Eq. (2) with speeds for the inner and outer wheels set as a percentage of the desired speed of the centre of mass.

Table II presents the results of 12 experiments for different settings of desired COM radii, COM speed and two settings of leg angles (seven laps were performed for each experiment). Desired radii and speed of the COM were matched to within approximately 10% for all experiments.

Roll-over stability is an important factor in the design of many wheeled vehicles, [21]. It should be noted that increasing

TABLE II  
EXPERIMENTAL RESULTS: TURNING

Exp #	Leg Angle [deg]	Outer Wheel Spds. [%]	Inner Wheel Spds. [%]	COM Speed Des.'d [m/s]	COM Speed Ach.'d [m/s]	Turn Radius Des.'d [m]	Turn Radius Ach.'d [m]
1	29.6	154, 141	56, 69	0.50	0.43	0.50	0.50
2	29.6	154, 141	56, 69	1.25	1.20	0.50	0.55
3	62.0	160, 147	58, 71	0.50	0.47	0.50	0.55
4	62.0	160, 147	58, 71	1.25	1.17	0.50	0.55
5	29.6	135, 127	70, 79	0.50	0.47	0.75	0.83
6	29.6	135, 127	70, 79	1.25	1.16	0.75	0.80
7	62.0	139, 131	72, 81	0.50	0.46	0.75	0.80
8	62.0	139, 131	72, 81	1.25	1.20	0.75	0.85
9	29.6	126, 120	78, 84	0.50	0.47	1.00	1.13
10	29.6	126, 120	78, 84	1.25	1.20	1.00	1.13
11	62.0	129, 123	79, 86	0.50	0.43	1.00	1.13
12	62.0	129, 123	79, 86	1.25	1.19	1.00	1.13

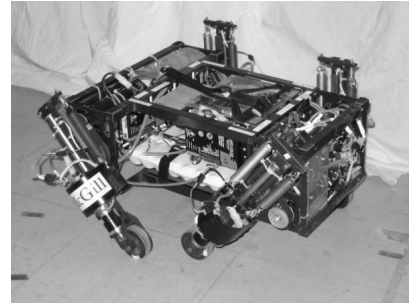
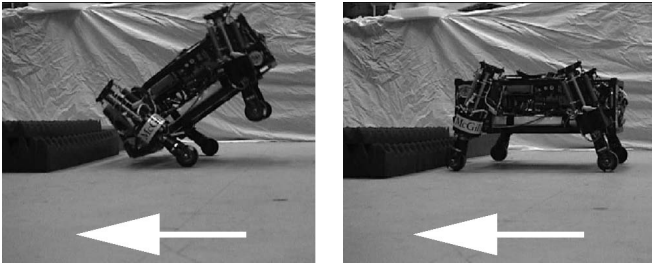


Fig. 3. The PAW robot executing an inclined turn.

the roll-over stability of the robot via the proposed and implemented turning algorithm is not critical at the speeds and radii of curvature it currently travels at, but it will become more important at higher speeds for this or a scaled-up version of the vehicle.

### D. Braking

To demonstrate the positive aspects of the braking algorithm described in Section III experimental trials were performed with the robot driving at 1.5 m/s and with the legs tucked in and sprawled out, alternatively using high and low control gains for the wheel motors (the hip motors used relatively high gains throughout). A summary of the experiments is found in Table III; ten runs were conducted for each setting and average braking distances were determined from these runs. In the first set of experiments the robot repeatedly tipped over while braking due to high gain wheel control and a tucked-in leg posture, as shown in Fig. 4a. In the second set of trials the wheel control gains were lowered and the robot



(a) Tipping over

(b) Stable braking

Fig. 4. Two different braking methods, one which leads to tipping the other which is stable. The robot is travelling from right to left.

did not tip over, but minor, non-critical, pitching is visible in video footage. A sprawled posture and high wheel gains, as conducted for the third set of experiments, resulted in wheel slip but a relatively short braking distance. In the fourth set of experiments, the wheel gains were lowered and a sprawled posture was used, as shown in Fig. 4b., yielded stable braking with little noticeable slip or pitching but with an increased braking distance.

TABLE III

EXPERIMENTAL RESULTS: BRAKING

Exp. #	Speed [m/s]	Leg Angle [deg]	Leg Angle Description	Controller Gains	Brake Dist. [m]
1	1.5	$\pm 11.5$	tucked	high	n/a
2	1.5	$\pm 11.5$	tucked	low	0.24
3	1.5	$\mp 11.5$	sprawled	high	0.15
4	1.5	$\mp 11.5$	sprawled	low	0.23

What these experiments demonstrate is that by simply decreasing the wheel control gains it is possible to reduce sliding and critical pitching motion during braking, while increasing braking distance. Using a sprawled posture further increases the stability of the robot, reducing pitching motion during braking in both low and high gain wheel control modes.

## V. CONCLUSIONS & FUTURE WORK

This paper presented current wheeled mobility work on a hybrid wheeled-leg robot called PAW. Design details and controllers for inclined turning and sprawled braking, which take advantage of the hybrid nature of the platform and improve stability were discussed. The robot demonstrated straight-line rolling at up to 2.0 m/s and performed turns by taking advantage of the ability to reconfigure wheel placement. In addition, through appropriate wheel placement and low controller gains the robot demonstrated the ability to brake without tipping over. Power consumption values were measured and an operational range of over 2500 m in one hour was determined.

Work is currently being performed on legged and inertial-based rolling behaviours and will be presented in the future.

## ACKNOWLEDGMENTS

The authors would like to thank a number of people who have been involved in the PAW project, particularly Martin Buehler and Carl Steeves, as well as Don Campbell, Dave Cowan, Philippe Giguère, Michelle Huth, Julien Marcil, Dave McMordie, Neil Neville, Ioannis Poulakakis, Chris Prahacs,

Enrico Sabelli, Aaron Saunders, Shane Saunderson, John Sheldon, and Mike Tolley. James A. Smith's work has been made possible through support from Defence R&D Canada.

## REFERENCES

- [1] M. G. Bekker. *Introduction to Terrain-Vehicle Systems*. University of Michigan Press, Ann Arbor, MI, USA, 1969.
- [2] J. Y. Wong. *Theory of Ground Vehicles*. John Wiley, New York, New York, USA, 3rd edition, 2001.
- [3] K. Iagnemma and S. Dubowsky. *Mobile Robots in Rough Terrain Estimation, Motion Planning, and Control With Application to Planetary Rovers*, Volume 12 of Springer Tracts in Advanced Robotics. Springer, New York, USA, 2004.
- [4] B. L. Digney and S. Penzes. "Robotic Concepts for Urban Operations." In *Proceedings of SPIE, Unmanned Ground Vehicle Technology IV*, Volume 4715, pp 63 - 74, 2002.
- [5] B. McBride, R. Longoria, and E. Krotkov. "Measurement and Prediction of the Off-Road Mobility of Small Robotic Ground Vehicles." In *The 3rd Performance Metrics for Intelligent Systems Workshop (PerMISO3)*, Gaithersburg, MD, USA, 2003. National Institute of Standards and Technology.
- [6] T. Frost, C. Norman, S. Pratt, B. Yamauchi, B. McBride, and G. Peri. "Derived Performance Metrics and Measurements Compared to Field Experience for the Packbot." In *Measuring the Performance and Intelligence of Systems: Proceedings of the 2002 PerMIS Workshop*. National Institute of Standards and Technology, August 2002.
- [7] A. Mishkin. *Sojourner: An Insider's View of the Mars Pathfinder Mission*. Berkley Publishing Group, 2003.
- [8] T. A. McMahon. *Muscles, Reflexes, and Locomotion*. Princeton University Press, Princeton, N.J., USA, 1984.
- [9] S.-M. Song and K. J. Waldron. *Machines That Walk: The Adaptive Suspension Vehicle*. MIT Press, Cambridge, Massachusetts, 1989.
- [10] M. Raibert. *Legged Robots That Balance*. The MIT Press, Cambridge, MA, USA, 1986.
- [11] K. Autumn, M. Buehler, M. Cutkosky, R. Fearing, R. J. Full, D. Goldman, R. Groff, W. Provancher, A. E. Rizzi, U. Saranli, A. Saunders and D. Koditschek. "Robotics in Scansorial Environments." In *Proceedings of SPIE*, Vol. #5804, pp. 291-302, 2005.
- [12] I. Poulakakis, J. A. Smith, and M. Buehler. "Modeling and Experiments of Untethered Quadrupedal Running With a Bounding Gait: The Scout II Robot." *International Journal of Robotics Research*, 24: 239 - 256, April 2005.
- [13] U. Saranli, M. Buehler, and D. E. Koditschek. "RHex: A Simple and Highly Mobile Hexapod Robot." *International Journal of Robotics Research*, 20(7): 616 - 631, 2001.
- [14] T. Estier, Y. Crausaz, B. Merminod, M. Lauria, R. Piguët and R. Siegwart. "An Innovative Space Rover With Extended Climbing Abilities." In *Proceedings of Space and Robotics 2000*, Albuquerque, USA, February 27 - March 2, 2000.
- [15] C. Grand, F. Benamar, F. Plumet, and P. Bidaud. "Stability and Traction Optimization of a Reconfigurable Wheel-Legged Robot." *International Journal of Robotics Research*, 23(10-11):1041-1058, 2004.
- [16] G. Endo and S. Hirose. "Study on Roller-Walker (Multi-Mode Steering Control and Self-Contained Locomotion)." In *Proceedings of the IEEE International Conference on Robotics and Automation (ICRA)*, 2000., pp. 2808 - 2814, San Francisco, CA, USA, 2000.
- [17] C. Steeves. *Design and Behavioural Control of a Dynamic Quadruped With Active Wheels*. Masters Thesis, McGill University, November 2002.
- [18] D. McMordie, C. Prahacs, and M. Buehler. "Towards a Dynamic Actuator Model for a Hexapod Robot." In *Proceedings of the International Conference on Robotics and Automation (ICRA)*, pp. 1386 - 1390, Taipei, Taiwan, 2003.
- [19] J. Angeles. *Fundamentals of Robotic Mechanical Systems - Theory, Methods, and Algorithms*. Springer-Verlag, Second edition, June 2001.
- [20] G. Gabrielli and T. H. von Karman. "What Price Speed? : Specific Power Required for Propulsion of Vehicles." *Mechanical Engineering*, 72(10): 775 - 781, 1950.
- [21] D. J. M. Sampson. *Active Roll Control of Articulated Heavy Vehicles*. PhD Thesis, University of Cambridge, 2000.
- [22] J. A. Smith and I. Poulakakis. "Rotary Gallop in the Untethered Quadrupedal Robot Scout II." In *Proceedings of the 2004 IEEE/RSJ International Conference on Intelligent Robots and Systems (IROS)*, Sendai, Japan, 2004.